

Supplementary Information

**Ultrathin Co-Fe Hydroxide Nanosheet Arrays for Improved
Oxygen Evolution during Water Splitting**

Tingting Zhou,^[a,b] Zhen Cao,^[a] Heng Wang,^[a] Zhen Gao,^[a] Long Li,^[a] Houyi Ma^[b] and Yunfeng Zhao^{[a]*}

- a. Tianjin Key Laboratory of Advanced Functional Porous Materials, Institute for New Energy Materials and Low-Carbon Technologies, Tianjin University of Technology, Tianjin 300384, China School of Chemistry and
- b. Chemical Engineering, Shandong University, Jinan 250100, China.

Table S1. ICP results of $\text{Co}_y\text{Fe}_{1-y}(\text{OH})_x$ NSAs.

Number	Feed ratio of Co:Fe	Content of Co (mg/cm ²)	Content of Fe (mg/cm ²)	Atom ratio (Co : Fe)	y
1	1:0	0.37	0	----	1
2	3:1	0.38	0.13	1:0.34	0.75
3	2:1	0.39	0.16	1:0.41	0.7
4	1:1	0.28	0.23	1:0.82	0.55
5	1:2	0.22	0.31	1:1.40	0.41
6	0:1	0	0.39	----	0

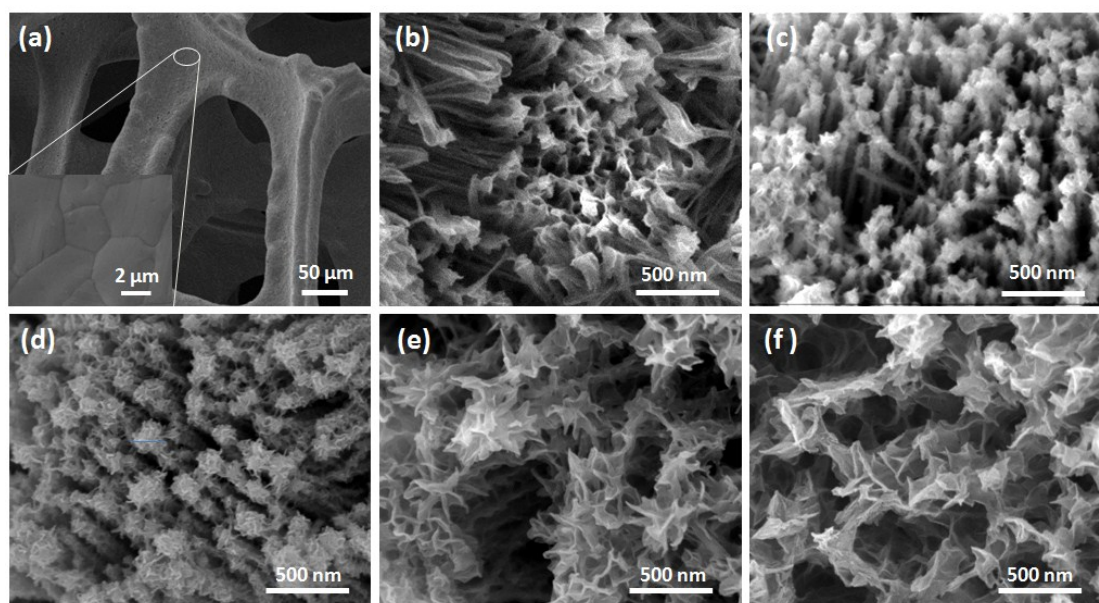


Fig. S1. SEM images of (a) foam Cu, (b) Co(OH)_2 NSAs, (c) $\text{Co}_{0.75}\text{Fe}_{0.25}(\text{OH})_x$ NSAs, (d) $\text{Co}_{0.55}\text{Fe}_{0.45}(\text{OH})_x$ NSAs, (e) $\text{Co}_{0.41}\text{Fe}_{0.59}(\text{OH})_x$ NSAs and (f) Fe(OH)_x NSAs.

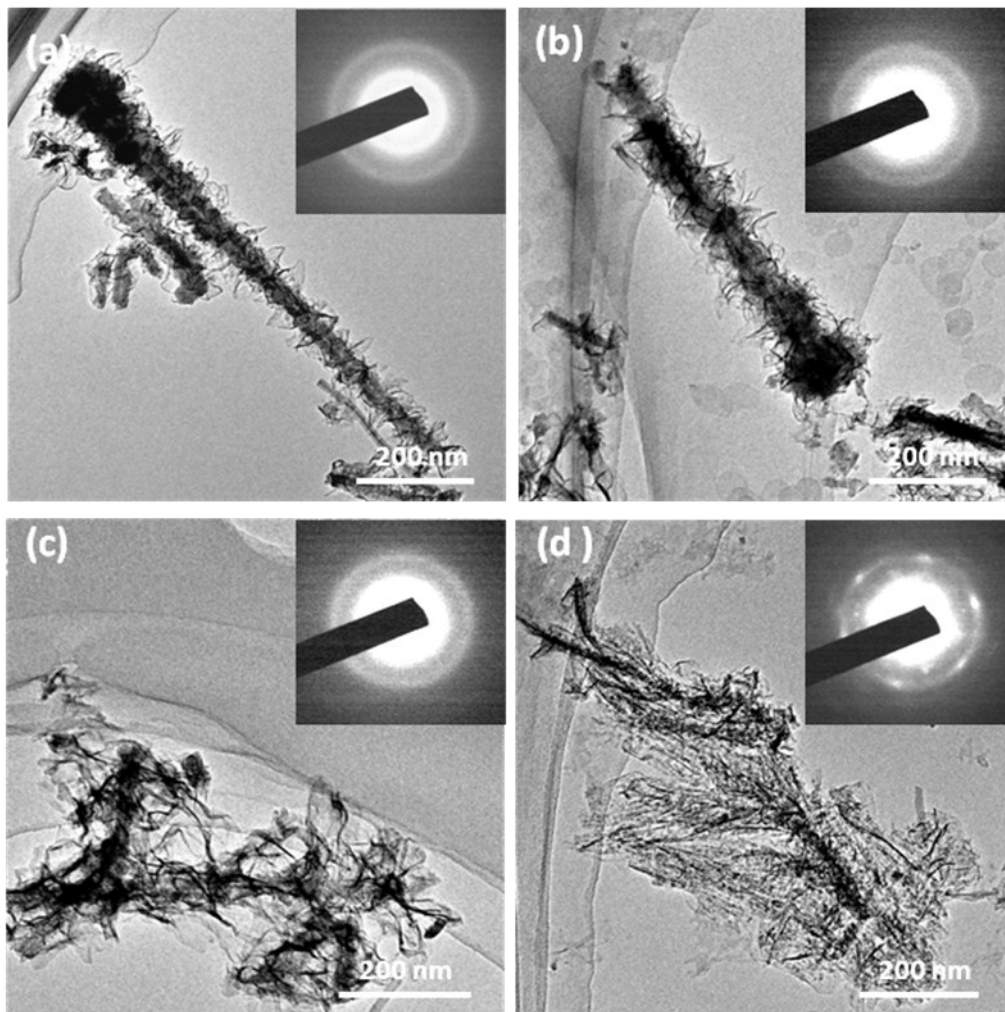


Fig. S2. TEM images and (inset) SAED patterns of (a) $\text{Co}_{0.75}\text{Fe}_{0.25}(\text{OH})_x$ NSAs, (b) $\text{Co}_{0.55}\text{Fe}_{0.45}(\text{OH})_x$ NSAs, (c) $\text{Co}_{0.41}\text{Fe}_{0.59}(\text{OH})_x$ NSAs and (d) Fe_2O_3 NSAs.

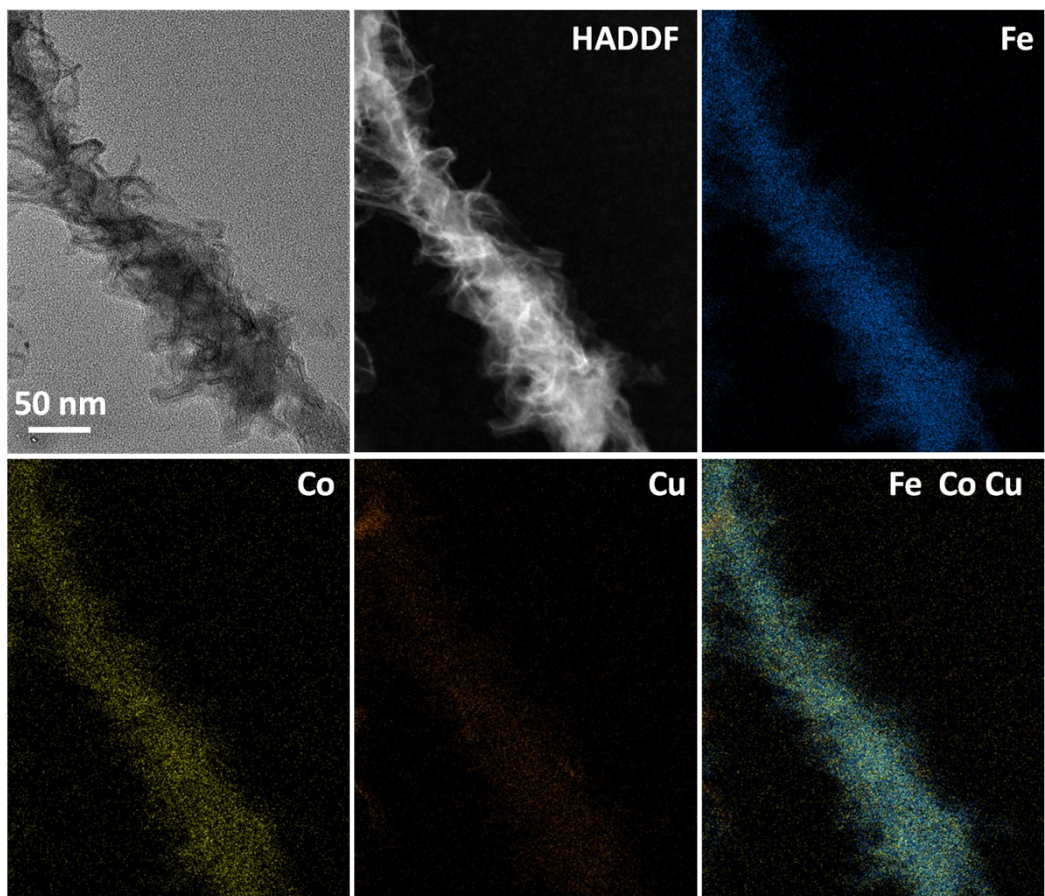


Fig. S3. The TEM image and corresponding Co, Fe and Cu EDS mapping images of $\text{Co}_{0.70}\text{Fe}_{0.30}(\text{OH})_x$ NSAs.

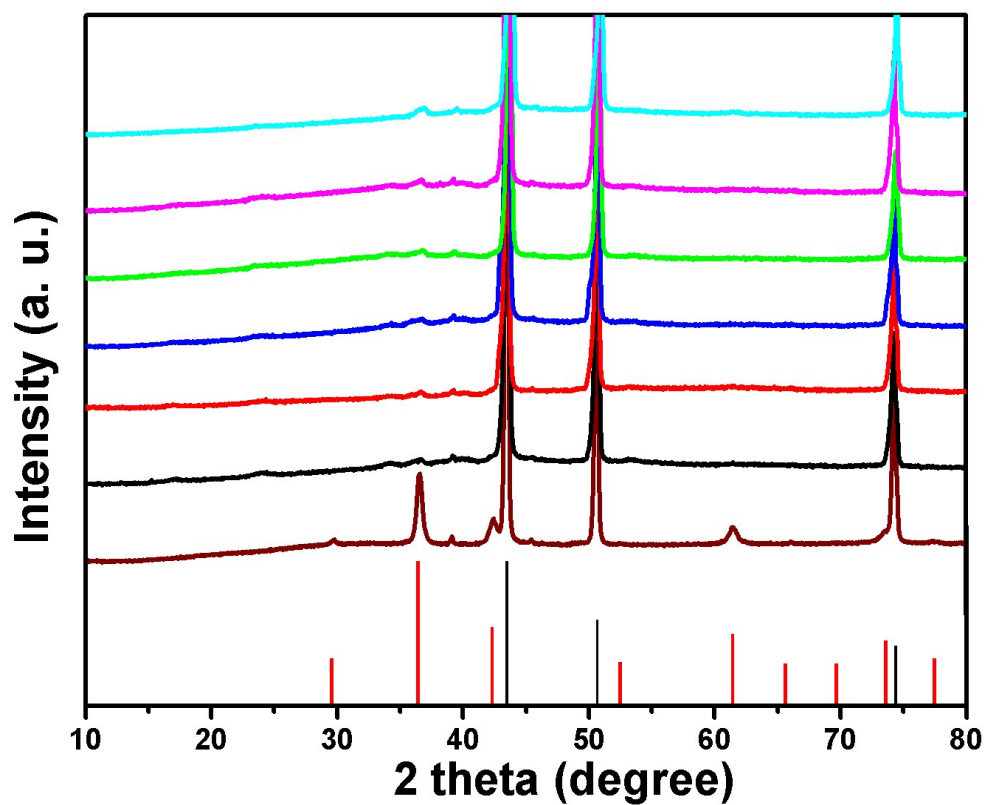


Fig. S4. XRD patterns for Cu₂O template, Co(OH)₂, Co_{0.75}Fe_{0.25}(OH)_x, Co_{0.70}Fe_{0.30}(OH)_x, Co_{0.55}Fe_{0.45}(OH)_x, Co_{0.41}Fe_{0.59}(OH)_x and Fe₂O₃ NSAs (lines from bottom to top). The peaks are indexed using reference peaks from the appropriate PDF cards: Cu₂O phases (red, PDF#65-3288) and Cu phases (black, PDF# 65-9743).

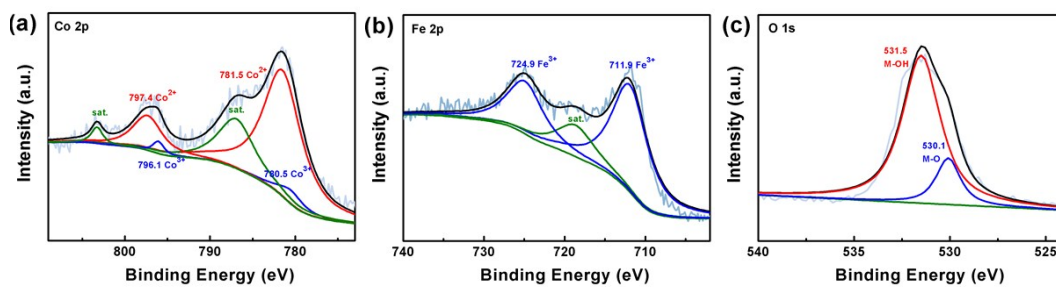


Fig. S5. High-resolution XPS spectra of (a) Co 2p, (b) Fe 2p and (c) O 1s of $\text{Co}_{0.75}\text{Fe}_{0.25}(\text{OH})_x$ NSAs.

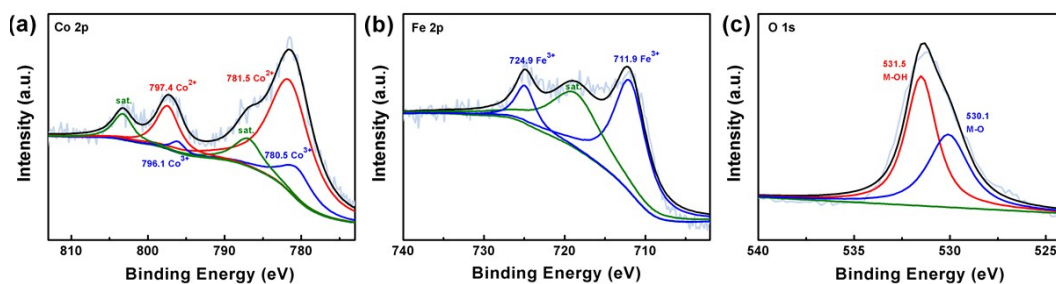


Fig. S6. High-resolution XPS spectra of (a) Co 2p, (b) Fe 2p and (c) O 1s of $\text{Co}_{0.55}\text{Fe}_{0.45}(\text{OH})_x$ NSAs.

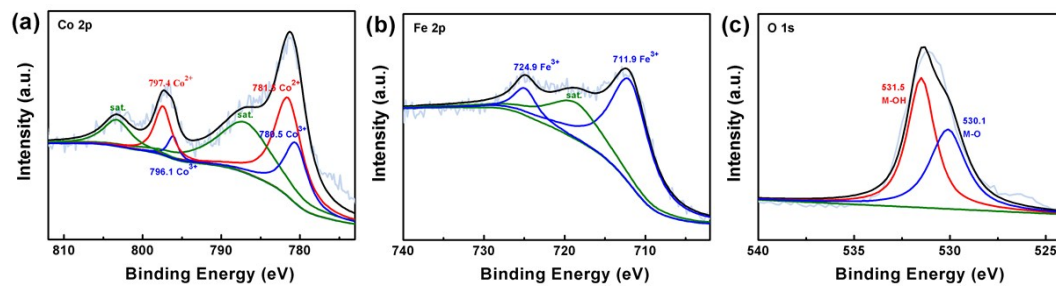


Fig. S7. High-resolution XPS spectra of (a) Co 2p, (b) Fe 2p and (c) O 1s of $\text{Co}_{0.41}\text{Fe}_{0.59}(\text{OH})_x$ NSAs.

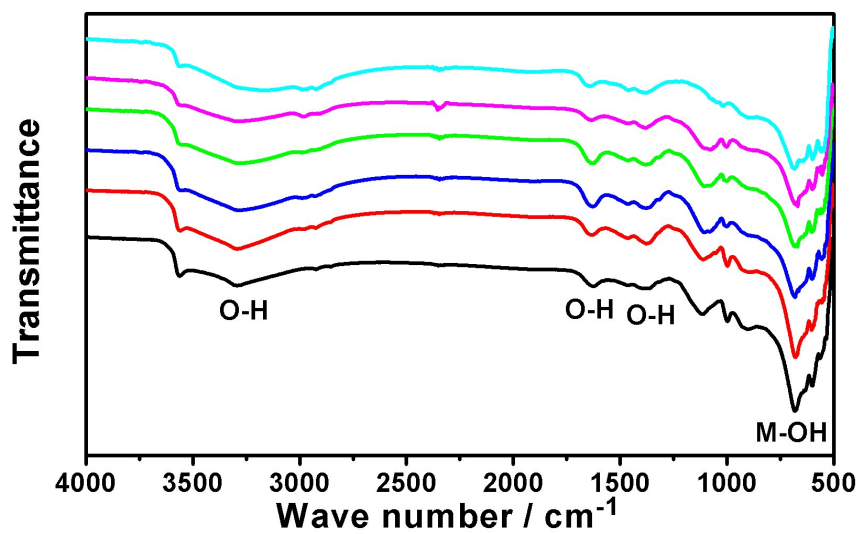


Fig. S8. Infrared spectra of $\text{Co}(\text{OH})_2$, $\text{Co}_{0.75}\text{Fe}_{0.25}(\text{OH})_x$, $\text{Co}_{0.70}\text{Fe}_{0.30}(\text{OH})_x$, $\text{Co}_{0.55}\text{Fe}_{0.45}(\text{OH})_x$, $\text{Co}_{0.41}\text{Fe}_{0.59}(\text{OH})_x$ and Fe_2O_3 NSAs (lines from bottom to top).

Table S2. OER catalytic performances of $\text{Co}_y\text{Fe}_{1-y}(\text{OH})_x$ NSAs in 1 M KOH.

Catalyst	Onset η (mV)	η at 10 mA cm ⁻² (mV)	η at 100 mA cm ⁻² (mV)	Tafel Slope (mV/dec)	TOF at $\eta=380$ mV (s ⁻¹)
Co(OH)₂	250	270	347	74.9	0.081
Co_{0.75}Fe_{0.25}(OH)_x	235	250	320	67.3	0.103
Co_{0.70}Fe_{0.30}(OH)_x	220	245	310	62.4	0.172
Co_{0.55}Fe_{0.45}(OH)_x	220	248	315	65.4	0.126
Co_{0.41}Fe_{0.59}(OH)_x	225	262	330	68.9	0.076
Fe₂O₃	270	325	375	50.9	0.045

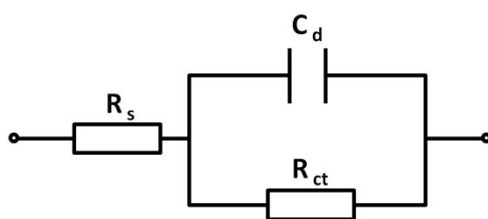


Fig. S9. Equivalent circuit used for fitting the EIS data.

Table S3. Fitting results of $\text{Co}_y\text{Fe}_{1-y}(\text{OH})_x$ NSAs.

Material	R_s (Ω)	R_{ct} (Ω)	R_{cp} (Ω)
$\text{Co}(\text{OH})_2$	2.22	3.57	0.21
$\text{Co}_{0.75}\text{Fe}_{0.25}(\text{OH})_x$	3.62	4.08	0.09
$\text{Co}_{0.70}\text{Fe}_{0.30}(\text{OH})_x$	3.20	2.91	0.16
$\text{Co}_{0.55}\text{Fe}_{0.45}(\text{OH})_x$	2.74	3.53	8.12
$\text{Co}_{0.41}\text{Fe}_{0.59}(\text{OH})_x$	3.18	9.64	3.68
Fe_2O_3	3.74	24.4	0.089

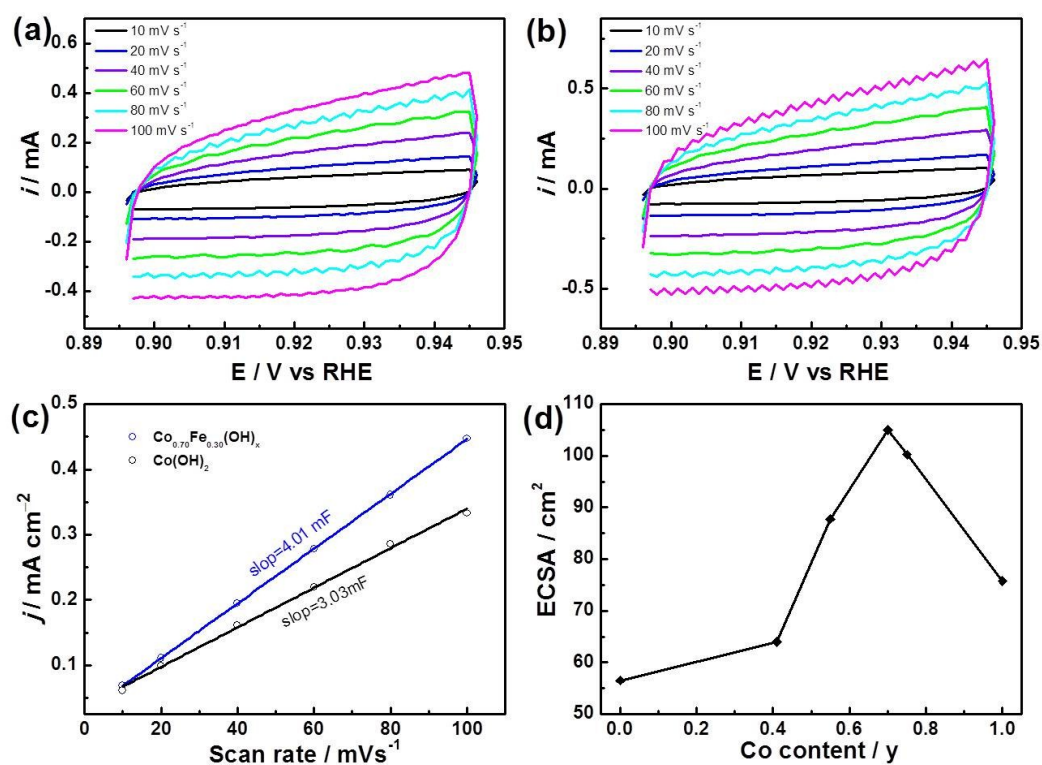


Fig. S10. Cyclic voltammetry curves of (a) Co(OH)₂ and (b) Co_{0.70}Fe_{0.30}(OH)_x NSAs, (c) the cathodic charging currents measured at 0.92 V vs RHE plotted as a function of scan rate for Co(OH)₂ and Co_{0.70}Fe_{0.30}(OH)_x NSAs, (d) ECSA of Co_yFe_{1-y}(OH)_x NSAs.

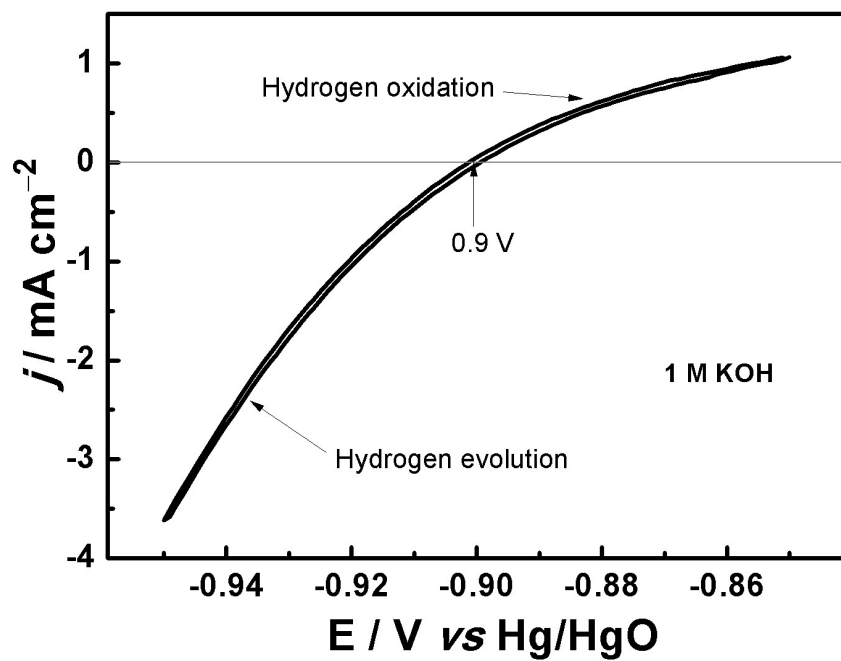


Fig. S11. Hg/HgO (1 M KOH) electrode calibrate with a 1M KOH solution.

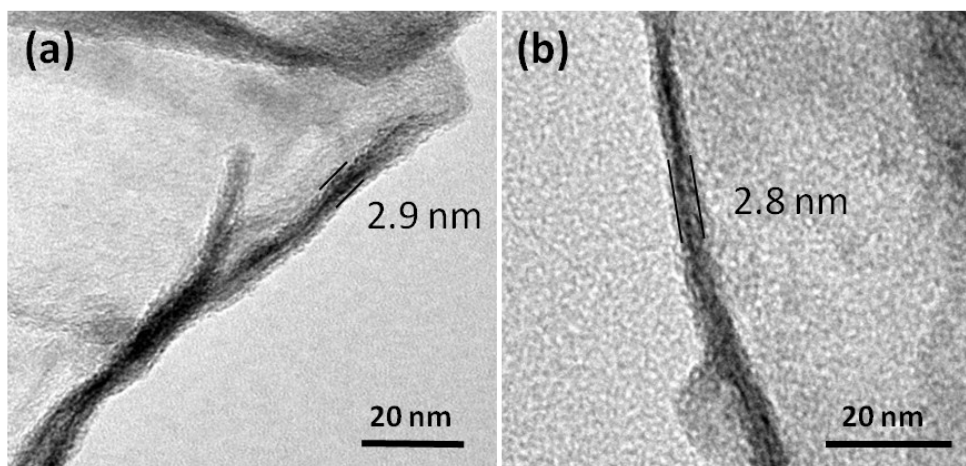


Fig. S12 TEM images of $\text{Co}_{0.70}\text{Fe}_{0.30}(\text{OH})_x$ NSAs edge curled nanosheets.

Table S4. The OER activities of some Co-based electrocatalysts for water oxidation under alkaline solution.

Catalyst	Electrolyte	Onset η (mV)	η at 10 mA cm ⁻² (mV)	Tafel Slope (mV dec ⁻¹)	TOF (s ⁻¹)	Mass loading (mg cm ⁻²)	Ref.
NiCo ₂ O ₄ core-shell nanowire	1 M NaOH	270	320	63.1	NA	NA	[1]
Mesoporous Ni sphere array	0.1 M KOH	190	254	39	0.0281 ($\eta=450$ mV)	0.2	[2]
Zn _x Co _{3-x} O ₄ nanoarrays	0.1 M KOH	NA	320	51	NA	0.2	[3]
Ni ₂ P nanowires	1.0 M KOH	310	400	60	NA	0.1	[4]
Co ₃ O ₄ Nanoparticles	1 M KOH	320	370	62	NA	0.325	[5]
Co ₃ O ₄ nanocube/CoO	1 M KOH	NA	430	89	NA	56.5	[6]
CoO _x nanotube	1 M KOH	230	NA	75	NA	0.136	[7]
Ni-V LDH	1 M KOH	250	300	50	0.054 ($\eta=350$ mV)	0.143	[8]
NiCoO _x hollow nanosponges	0.1 M KOH	271	362	73.2	NA	0.2	[9]
Screw CoNi LDH/C	1M KOH	330	360	38.5	NA	2	[10]
NiCo/NF or NiCo/CP	1 M KOH	NA	360	50-60	NA	0.4	[11]
NiCoO _x nanoarray	1 M KOH	280	290	79	NA	3	[12]
Co-S nanosheets film	1 M KOH	320	361	64	NA	NA	[13]
NiCo hydroxide	0.1 M KOH	310	460	65	NA	NA	[14]
Hollow fluffy cages	1 M KOH	NA	409	70	0.0167 ($\eta=400$ mV)	0.14	[15]
Ni _{2/3} Fe _{1/3} -rGO	1 M KOH	210	230	40	0.1 ($\eta=300$ mV)	0.25	[16]
Ni ₃ S ₂ nanorods/NF	0.1 M KOH	157	187	153	NA	NA	[17]
Fe-Ni/NF	1MKOH	200	NA	32	0.075 ($\eta=400$ mV)	NA	[18]
CoFe ₂ O ₄ nanoparticles	1M NaOH	270	378	73	NA	1.031	[19]
CoFe-LDH	0.1 M KOH	260	325	43	0.12 ($\eta=350$ mV)	0.2	[20]
FeOOH/Co/FeOOH Hybrid Arrays	1M NaOH	230	NA	32	5.6 ($\eta=300$ mV)	0.5	[21]

Notes and references

- [1] R. Chen, H.-Y. Wang, J. Miao, H. Yang and B. Liu, *Nano Energy* **2015**, *11*, 333-340.
- [2] T. Sun, L. Xu, Y. Yan, A. A. Zakhidov, R. H. Baughman and J. Chen, *ACS Catal.* **2016**, *6*, 1446-1450.
- [3] X. Liu, Z. Chang, L. Luo, T. Xu, X. Lei, J. Liu and X. Sun, *Chem. Mater.* **2014**, *26*, 1889-1895.
- [4] A. Han, H. Chen, Z. Sun, J. Xu and P. Du, *Chem. Commun.* **2015**, *51*, 11626-11629.
- [5] Xinzhe Li, Yiyun Fang, Xiaoqing Lin, Min Tian, Xingcai An, Yan Fu, Rong Li, Jun Jina and J. Maa, *J. Mater. Chem. A* **2015**, *3*, 17392-17402.
- [6] A. Bergmann, E. Martinez-Moreno, D. Teschner, P. Chernev, M. Gliech, J. F. de Araujo, T. Reier, H. Dau and P. Strasser, *Nat. Commun.* **2015**, *6*, 8625.
- [7] Y. Wang, K. Jiang, H. Zhang, T. Zhou, J. Wang, W. Wei, Z. Yang, X. Sun, W.-B. Cai and G. Zheng, *Adv. Sci.* **2015**, *2*, 1500003.
- [8] K. Fan, H. Chen, Y. Ji, H. Huang, P. M. Claesson, Q. Daniel, B. Philippe, H. Rensmo, F. Li, Y. Luo and L. Sun, *Nat Commun* **2016**, *7*, 11981.
- [9] C. Zhu, D. Wen, S. Leubner, M. Oschatz, W. Liu, M. Holzschuh, F. Simon, S. Kaskelb and A. Eychmuller, *Chem. Commun.* **2015**, *51*, 7851--7854.
- [10] B. Ni and X. Wang, *Chem. Sci.* **2015**, *6*, 3572-3576.
- [11] Y. Xiao, L. Feng, C. Hu, V. Fateev, C. Liu and W. Xing, *RSC Adv.* **2015**, *5*, 61900-61905.
- [12] Z. Lu, M. Sun, T. Xu, Y. Li, W. Xu, Z. Chang, Y. Ding, X. Sun and L. Jiang, *Adv. Mater.* **2015**, *27*, 2361-2366.
- [13] T. Liu, Y. Liang, Q. Liu, X. Sun, Y. He and A. M. Asiri, *Electrochem. Commun.* **2015**, *60*, 92-96.
- [14] Z. Zhao, H. Wu, H. He, X. Xu and Y. Jin, *Adv. Funct. Mater.* **2014**, *24*, 4698-4705.
- [15] X. Zhou, X. Shen, Z. Xia, Z. Zhang, J. Li, Y. Ma and Y. Qu, *ACS Appl. Mater. Inter.* **2015**, *7*, 20322-20331.
- [16] M. Wei, M. Renzhi, W. Chengxiang, L. Jianbo, L. Xiaohe, Z. Kechao and T. Sasaki, *ACS Nano* **9**, 1977-1984.
- [17] W. Zhou, X.-J. Wu, X. Cao, X. Huang, C. Tan, J. Tian, H. Liu, J. Wang and H. Zhang, *Energy. Environ. Sci.* **2013**, *6*, 2921.
- [18] X. Lu and C. Zhao, *Nat. Commun.* **2015**, *6*, 6616.
- [19] A. Kargar, S. Yavuz, T. K. Kim, C. H. Liu, C. Kuru, C. S. Rustomji, S. Jin and P. R. Bandaru, *ACS Appl. Mater. Inter.* **2015**, *7*, 17851-17856.
- [20] X. Han, C. Yu, J. Yang, C. Zhao, H. Huang, Z. Liu, P. M. Ajayan and J. Qiu, *Adv. Mater. Interface.* **2016**, *3*, 15000782.
- [21] J. X. Feng, H. Xu, Y. T. Dong, S. H. Ye, Y. X. Tong and G. R. Li, *Angew. Chem. Int. Ed.* **2016**, *55*, 3694-3698.